

| | |
|--------------|---|
| Title | Effect of thermal degradation on rheological properties for poly(3-hydroxybutyrate) |
| Author(s) | Yamaguchi, M; Arakawa, K. |
| Citation | European Polymer Journal, 42(7): 1479-1486 |
| Issue Date | 2006-07 |
| Type | Journal Article |
| Text version | author |
| URL | http://hdl.handle.net/10119/3381 |
| Rights | Elsevier Ltd., Masayuki Yamaguchi and Keiichi Arakawa, European Polymer Journal, 42(7), 2006, 1479-1486. http://www.sciencedirect.com/science/journal/00143057 |
| Description | |

Effect of Thermal Degradation on Rheological Properties for Poly(3-hydroxybutyrate)

Masayuki Yamaguchi and Keiichi Arakawa

School of Materials Science,
Japan Advanced Institute of Science and Technology
1-1 Asahidai, Nomi, Ishikawa 923-1292 JAPAN

Corresponding to
Masayuki Yamaguchi
School of Materials Science, Japan Advanced Institute of Science and Technology
1-1 Asahidai, Nomi, Ishikawa 923-1292 Japan
Phone +81-761-51-1621, Fax +81-761-51-1625
E-mail m_yama@jaist.ac.jp

ABSTRACT: Thermal degradation at processing temperature and the effect on the rheological properties for poly(3-hydroxybutyrate) have been studied by means of oscillatory shear modulus and capillary extrusion properties, with the aid of molecular weight measurements. Thermal history at processing temperature depresses the viscosity because of random chain scission. As a result, gross melt fracture hardly takes place with increasing the residence time in a capillary rheometer. Moreover, it was also found that the molecular weight distribution is independent of the residence time, whereas the inverse of the average molecular weight is proportional to the residence time. Prediction of average molecular weight with a constant molecular weight distribution makes it possible to calculate the flow curve following generalized Newtonian fluid equation proposed by Carreau as a function of temperature as well as the residence time.

Key words: poly(3-hydroxybutyrate); rheological properties;
thermal degradation

INTRODUCTION

Poly(3-hydroxybutyrate) (PHB) and its copolymer have been known as one of the most famous biopolyesters since the success of isolation and identification in 1926.¹ Although the first trial to commercialization, which started in the late 1980s,² did not result in the major replacement from conventional plastics because of the poor cost-performance and the lack of thermal stability, PHB and its copolymer have received increasing attention these days owing to the rapid growth of the interest in environment. The thermal degradation of PHB during processing, which is obvious beyond 170 °C, occurs even at lower temperature than the melting point of PHB homopolymer, 177 °C. Hence, considerable effort has been carried out to develop copolymers with 3-hydroxyvalerate, 4-hydroxybutyrate, or 3-hydroxyhexanoate in order to lower the melting point, and thus, the processing temperature,²⁻⁴ although the copolymerization loses the rigidity.

Pioneering work on thermal degradation of PHB has been carried out by Grassie et al.⁵⁻⁷ at various temperatures. They clarified the main reaction occurred at processing temperature, *i.e.*, between 170 and 200 °C, is a random chain scission,⁶ whereas the low molecular weight compounds are mainly generated by the thermal degradation beyond 300 °C.⁵ The random chain scission occurs at ester group, leading to the formation of carboxyl groups and vinyl crotonate ester groups, through six-membered ring ester decomposition process,^{6,7} which was proved by Kunioka and Doi by NMR measurements.⁸ Because of the simple first-order reaction, the inverse of number-average degree of polymerization for the sample is proportional to the residence time t at processing temperature.^{6,8} Moreover, Kunioka and Doi also demonstrated that apparent activation energy of thermal degradation is about 212 kJ/mol, which is independent of the copolymerization with 3-hydroxyvalerate or 4-hydroxybutyrate.⁸ Later, Daly et al, also evaluated the activation energy from the viscous depression, *i.e.*, rheological characterization, and obtained a similar level of activation energy, 190 kJ/mol.⁹ Moreover, Melik and Schechtman found that the degradation rate during processing is basically independent of the applied shear rate, although temperature rise due to viscous energy dissipation has an influence on the decomposition.¹⁰ Except for the study by Daly et al. and Melik and Schechtman, however, the rheological properties of PHB homopolymer

were not investigated in detail because of the complexity attributed to the thermal instability. The uncertainty of the rheological properties during processing is a serious problem to operate a processing machine appropriately, and thus, results in poor processability.

In this study, the linear viscoelastic properties as well as the capillary extrusion properties were evaluated at processing temperature considering the change of molecular weight. Further, it is shown that the flow curves during processing are predictable as a function of the residence time and the resin temperature. The results will have a great impact on the material design for PHB homopolymer, because it makes easier to control the processability and the mechanical properties of final products.

EXPERIMENTAL

Materials

The polymer employed in this study was microbial poly(3-hydroxybutyrate) homopolymer kindly supplied by PHB Industrial S/A in Brazil. The sample was compressed into a flat sheet by a compression-molding machine (Tester Sangyo, SA303IS) at 180 °C for 3 min. After cutting the obtained sheet, various rheological properties were evaluated.

Measurements

Oscillatory shear moduli, such as shear storage modulus G' and loss modulus G'' , were measured by a cone-and-plate rheometer (UBM, MR500) at various frequencies as a function of the residence time in the rheometer under a nitrogen atmosphere at 180 °C. The cone angle is 2 degree and the diameter of the cone is 25 mm. After setting the sample immediately between the cone and the plate, which were heated previously, we collected the oscillatory shear modulus. In this experiment, the Lissajous pattern can be regarded as closed ellipsoids even at the lowest frequency. We defined $t = 0$ after 2 min of residence in the rheometer. Further, extrusion properties, such as apparent shear stress and appearance of extrudates, have been investigated by a capillary rheometer (Yasuda Seiki Seisakusyo, Capillary Rheometer 140 SAS-2002) also as a function of the thermal history, *i.e.*, the residence time in the capillary rheometer, at an

apparent shear rate of 6.3 s^{-1} . The capillary die employed was 8 mm in length and 2.095 mm in diameter with an entrance angle of $\pi/2$. The temperature of the capillary reservoir cylinder was kept at $180 \text{ }^\circ\text{C}$. We again defined $t = 0$ at 2 min after putting the sample into the capillary rheometer. Details in the experimental method about the relation between residence time and rheological properties were described in the previous papers.^{11,12}

Molecular weight and its distribution were evaluated by a gel permeation chromatograph, g.p.c., (Tosoh, HLC-8020) with TSK-GEL® GMHXL, as a polystyrene standard. The thermal history of the sample was applied by the cone-and-plate rheometer at $180 \text{ }^\circ\text{C}$ following the method of the oscillatory measurement. Chloroform was employed as eluant at $40 \text{ }^\circ\text{C}$ at a flow rate of 1.0 ml/min and the concentration of the sample was 1.0 mg/ml. The g.p.c. characterization was carried out ignoring the oligomer fraction whose molecular weight is quite different from the main fraction, since the amount of the oligomer was quite less and independent of the thermal history in this experiment.

RESULTS

Oscillatory Shear Modulus

Because of chain scission, molecular weight and thus oscillatory modulus decrease with the residence time in the rheometer at $180 \text{ }^\circ\text{C}$ as exemplified in Figure 1.

[Figure 1], [Figure 2]

The depression is more obvious at a lower frequency, demonstrating longer relaxation time mechanism ascribed to higher molecular weight fraction becomes weak with increasing the thermal history. Further, the figure indicates that it is impossible to obtain the frequency dependence of oscillatory shear modulus by a conventional frequency sweep experiment at $180 \text{ }^\circ\text{C}$. Therefore, collecting the time variation of oscillatory moduli at various frequencies, we compose the viscoelastic curves as a function of frequency as shown in Figure 2. The figures demonstrate that applied thermal history significantly affects the rheological properties even for a short time, which is comparable with a residence time in a conventional processing machine, such as a

single-screw extruder and an injection-molding machine. Moreover, three curves of G' and G'' at various residence times in Figure 2 are superposed each other by only horizontal shift as illustrated in Figure 3, suggesting that thermal degradation does not affect molecular weight distribution. Further, the master curve also indicates that neither branching nor gelation occurs.

[Figure 3]

Capillary Extrusion

Depression of molecular weight, of course, affects the appearance of extrudates as well as the apparent shear stress at capillary flow. Figure 4 shows the time variation of the apparent shear stress σ at an apparent shear rate of 6.3 s^{-1} . It is found from the figure that the apparent shear stress decreases rapidly. The shear stress is a bit larger than the complex stress measured by oscillatory shear modulus, because neither Bagley nor Rabinowitsch corrections are carried out.

[Figure 4]

Figure 5 shows optical photographs of the strands extruded by the capillary rheometer at $180 \text{ }^\circ\text{C}$. As seen in the appearance of the strands shown in the top of the figure, some extrudates are characterized as wavy shape known as typical distortion pattern of gross, chaotic, volumetric melt fracture,¹²⁻¹⁶ which becomes obscure with increasing the residence time. The results are plausible because the gross melt fracture often takes place when the melt elasticity, which increases with molecular weight, is enhanced.¹²⁻¹⁶ Further, the strand with the residence time of 10 min cannot hold itself because of less drawdown force. Therefore, the strand falls down by its own weight. Moreover, it should be noted that the surface roughness of the strands shown in the bottom of the figure, which is similar to shark-skin failure reported by Zhu et al. employing poly(3-hydroxybutyrate-co-3-hydroxyvalerate),¹⁷ is also improved with the residence time. The improvement of surface roughness would be attributed to the reduction of shear stress.^{13-15,18}

[Figure 5]

The results of the capillary extrusion experiments demonstrate that the residence time in an extruder or an injection-molding machine has to be seriously taken into account at the evaluation of flow instability for PHB.

Molecular Weight

As demonstrated by Grassie et al.⁶ and Kunioka and Doi,⁸ the inverse of the number-average degree of polymerization $P_{N,t}$ at residence time t is given by the following relation because the main reaction is a random chain scission, *i.e.*, first-order reaction, at this temperature;

$$\frac{1}{P_{N,t}} - \frac{1}{P_{N,0}} = k_d t \quad (1)$$

where $P_{N,0}$ the initial number-average degree of polymerization and k_d the rate constant of thermal degradation, which is given by Arrhenius relation as follows;

$$k_d = A \exp\left(-\frac{\Delta H}{k_B T}\right) \quad (2)$$

where ΔH the activation energy for the reaction evaluated previously^{8,10} and k_B the Boltzmann constant.

The g.p.c. measurements in this study also confirm that the molecular weight of PHB follows equation (1) as shown in Figure 6, with a small deviation of the slope from the previous researches.^{6,8} Moreover, it was also found that g.p.c. curves do not change its shape with the residence time. Figure 7 shows the molecular weight distributions, such as M_w / M_n and M_z / M_w , as a function of the residence time. The g.p.c. results support the rheological properties in Figure 3.

[Figure 6] [Figure 7]

DISCUSSION

Figure 7 demonstrates that molecular weight distribution is almost independent of the residence time whereas the average molecular weight decreases rapidly. Equation (1) gives the number-average molecular weight as the following simple relation,

$$\frac{1}{M_{N,t}} = \frac{k_d t}{m} + \frac{1}{M_{N,0}} \quad (3)$$

where m is the molecular weight of the monomer unit.

Consequently, $M_{N,t}$ is written by;

$$M_{N,t} = \frac{1}{at + b} \quad (4)$$

where $a = k_d / m$ and $b = 1 / M_{N,0}$.

Further, considering M_w / M_N is constant, $M_{w,t}$ is expressed by the following relation;

$$M_{w,t} = \frac{c}{at + b} \quad (5)$$

where $c = M_w / M_N$.

The generalized Newtonian fluid (GNF) representation of the wall shear stress $\sigma(\dot{\gamma})$ is given by the product of shear rate $\dot{\gamma}$ and $\dot{\gamma}$ -dependent shear viscosity $\eta(\dot{\gamma})$ as,

$$\sigma(\dot{\gamma}) = \eta(\dot{\gamma}) \dot{\gamma} \quad (6)$$

According to the Carreau GNF equation,^{19,20} shear viscosity of GNF is expressed by

$$\eta(\dot{\gamma}) = \eta_0 \left[1 + (\tau_w \dot{\gamma})^2 \right]^{\frac{n-1}{2}} \quad (7)$$

where η_0 the zero-shear viscosity, n ($0 < n < 1$) the dimensionless parameter dependent on molecular weight distribution, and τ_w the weight-average relaxation time defined by equation (8).

$$\tau_w \equiv \frac{\int \tau^2 H(\tau) d \ln \tau}{\int \tau H(\tau) d \ln \tau} = \eta_0 J_e^0 \quad (8)$$

where $H(\tau)$ the relaxation spectrum and J_e^0 the steady-state compliance.

When $\dot{\gamma} \gg \tau_w^{-1}$, equation (7) becomes a simple power law relation as,

$$\eta(\dot{\gamma}) = K \dot{\gamma}^{n-1} \quad (9)$$

where K is so-called consistency.²⁰

Because molecular weight distribution, and thus, n in equation (7), is assumed to be a constant value, the flow curve of η/η_0 versus $\tau_w \dot{\gamma}$ is independent of the residence time, whereas both η_0 and τ_w decrease rapidly. Accordingly, shear viscosity at the residence time t , $\eta(\dot{\gamma}, t)$, can be written as;

$$\eta(\dot{\gamma}, t) = \eta_0(t) \left[1 + \{ \tau_w(t) \dot{\gamma} \}^2 \right]^{\frac{n-1}{2}} \quad (10)$$

[Table I], [Figure 8]

Table I shows the weight-average molecular weights M_w and zero-shear viscosities η_0 at various residence times, $t = 0, 5$, and 10 min. It is found that η_0 is proportional to $M_w^{3.6}$, which is close to the well-known relation,²¹ *i.e.*, $\eta_0 \propto M_w^{3.4}$. Therefore, η_0 at $t = 0$ is estimated to be 7000 [Pa s]. A fitting curve following equation (10) with $\eta_0(0) = 7000$ [Pa s] is shown in Figure 8 with the experimental values of complex shear viscosity. The fitting curve, denoted by a solid line, gives $\tau_w = 0.5$ [s] and $n = 0.62$.

Considering the empirical relation, $J_e^0 \propto (M_z / M_w)^{3.4-3.7}$, suggested by Mill,²¹ τ_w is crudely proportional to $M_z^{3.6}$. Since M_z / M_w as well as M_w / M_N keeps a constant irrespective of the residence time as demonstrated in Figure 7, $M_{z,t}$ is given by;

$$M_{z,t} = \frac{d}{at + b} \quad (11)$$

where d/c is M_z / M_w .

Therefore, $\eta_0(t)$ and $\tau_w(t)$ at a residence time t are given by the initial values at $t = 0$, *i.e.*, $\eta_0(0)$ and $\tau_w(0)$, as follows;

$$\eta_0(t) = \eta_0(0) \left(\frac{b}{at + b} \right)^{3.4} \quad (12)$$

$$\tau_w(t) = \tau_w(0) \left(\frac{b}{at + b} \right)^{3.4} \quad (13)$$

Consequently, the flow curves of the PHB, which are the function of the residence time, are predictable from equations (10), (12), and (13), as long as $\eta_0(0)$ and $\tau_w(0)$ are given.

The predicted values by the equations are also plotted in Figure 8 denoted as dotted lines with the experimental data of complex shear viscosities represented as circles. The figure demonstrates that the change of flow curve during processing, *i.e.*, applied thermal history, is calculated quantitatively. Further, apparent activation energy of chain scission reaction reported by Kunioka and Doi and Daly et al. would make it possible to estimate the flow curve at various processing temperatures. Moreover, the expression in equation (10) will be widely available for PHB and its copolymers because microbial polyhydroxyalkanoates, including PHB homopolymer, has a similar molecular weight distribution,³ *i.e.*, a similar n .

CONCLUSION

Rheological properties for PHB homopolymer at processing temperature have been studied considering the chain scission reaction during processing. It was found that the oscillatory shear modulus and the steady-state shear stress decrease with the residence time in a rheometer in accord with the reduction of molecular weight. Further, the depression of shear stress and melt elasticity diminishes the onset of gross, chaotic melt fracture with surface roughness of the extrudates at capillary extrusion. Furthermore, the inverse of molecular weight is proportional to the residence time in a rheometer with a constant molecular weight distribution. Finally, the change in the flow curve due to thermal degradation at processing temperature is successfully predicted by Carreau's generalized Newtonian fluid model, which will give useful information on the actual processing for PHB and its copolymers.

Acknowledgement

The authors express their gratitude to PHB Industrial S/A in Brazil for their kind supply of the sample employed in the study.

REFERENCES

1. Lemoigne M. *Bull Soc Chem Biol* 1926;8:770.
2. Asrar J, Gruys KJ, Biodegradable Polymer Biopol, In: Doi Y, Steinbüchel A, editors. *Biopolymers Vol. 3b*. Wiley-VCH; 2002. chapter 3.
3. Abe H, Doi Y, Molecular and Material Design of Biodegradable Poly(hydroxyalkanoate)s, In: Doi Y, Steinbüchel A, editors. *Biopolymers Vol. 3c*. Wiley-VCH; 2002. chapter 5.
4. Satkowski MM, Melik DH, Autran J, Green PR, Noda I, Schechtman LA. Physical and Processing Properties of Polyhydroxyalkanoate Copolymers, In: Doi Y, Steinbüchel A, editors. *Biopolymers Vol. 3c*. Wiley-VCH; 2002. chapter 9.
5. Grassie N, Murray EJ, Holmes PA. *Polym Degrad Stab* 1984; 6:47.
6. Grassie N, Murray EJ, Holmes PA. *Polym Degrad Stab* 1984;6:95.
7. Grassie N, Murray EJ, Holmes PA. *Polym Degrad Stab* 1984;6:127.
8. Kunioka M, Doi Y. *Macromol* 1990;23:1933.
9. Daly PA, Bruce DA, Melik DH, Harrison GM. *J Appl Polym Sci* 2005;98:66.
10. Melik DH, Schechtman LA. *Polym Eng Sci* 1995;35:1795.
11. Yamaguchi M, Gogos CG. *Adv Polym Technol* 2001;20:261.
12. Yamaguchi M. *J Appl Polym Sci* 2001;82:1277.
13. Tordella JP. In: Erich FR, editor. *Rheology*. New York: Academic Press; 1969. p.57.
14. White JL. *Appl Polym Symp* 1973;20:155.
15. Cogswell FN. *Polymer Melt Rheology*. New York: Wiley; 1981.
16. Yamaguchi M, Todd DB, Gogos CG. *Adv Polym Technol* 2003;22:179.
17. Zhu Z, Dakwa P, Tapadia P, Whitehouse RS, Wang S. *Macromol* 2003;36:4891.
18. Yamaguchi M, Miyata H, Tan V, Gogos CG. *Polym* 2002;43:5249.
19. Carreau PJ. Ph.D. thesis, Univ. Wisconsin, 1968.
20. Tadmor Z, Gogos CG. *Principles of Polymer Processing*, New York: Wiley; 1979. chapter 6.
21. Ferry JD. *Viscoelastic Properties of Polymers*. New York: Wiley; 1980.

Figure Captions

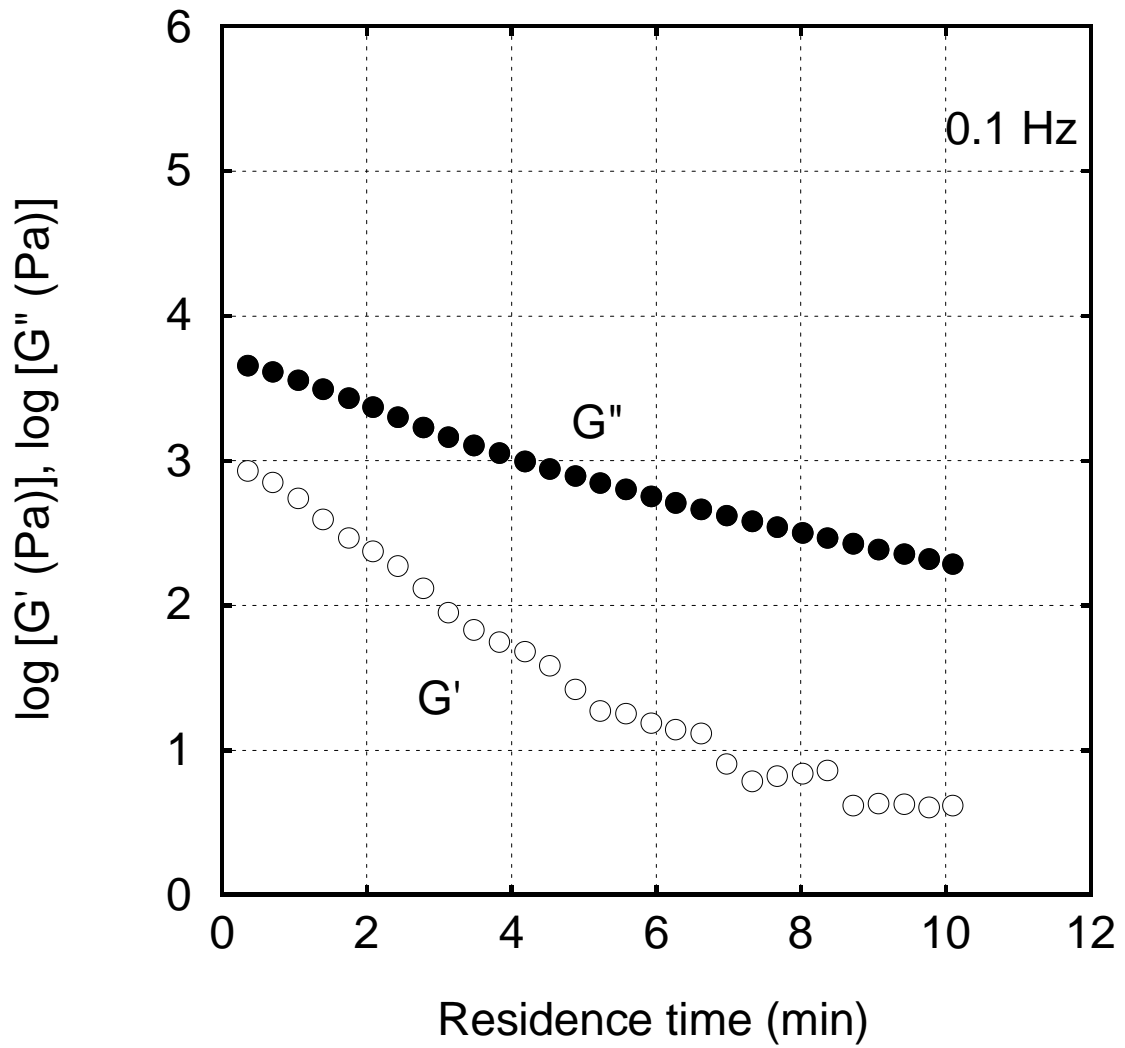
- Figure 1 Residence time dependence of shear storage modulus G' (\circ) and loss modulus G'' (\bullet) at 180 °C at (a) 0.1 Hz, (b) 1 Hz, and (c) 10 Hz for PHB.
- Figure 2 Shear storage modulus G' (\circ) and loss modulus G'' (\bullet) at 180 °C plotted against angular frequency ω for the samples with various residence times in the rheometer; (a) 0 min, (b) 5 min, and (c) 10 min.
- Figure 3 Master curves of shear storage modulus G' (open symbols) and loss modulus G'' (closed symbols) at 180 °C for the samples with various residence times in the rheometer; (circles) $t = 0$ min, (triangles) $t = 5$ min, and (diamonds) $t = 10$ min. a_D is the shift factor, and the residence time for the reference sample is 0 min, *i.e.*, $a_D = 1$.
- Figure 4 Apparent shear stress σ at a shear rate of 6.3 s^{-1} plotted against the residence time at 180 °C.
- Figure 5 Optical photographs of strands extruded from a capillary rheometer at a shear rate of 6.3 s^{-1} at 180 °C with various residence times.
- Figure 6 Inverse of number-average molecular weight, $1/M_N$, against the residence time in the rheometer at 180 °C.
- Figure 7 Molecular weight distribution, such as (circles) M_w/M_N and (diamonds) M_z/M_w , as a function of the residence time.
- Figure 8 Experimental data of absolute value of complex shear viscosity $\eta^*(\omega; t)$ for the sample with various residence times at 180 °C; circles $t = 0$ min, triangles $t = 5$ min, and diamonds $t = 10$ min. In the figure, a fitting curve by equation (10) with $\eta_0(0) = 7000 \text{ [Pa s]}$ is represented by a solid line. The

dotted lines are the predicted ones at $t = 5$ and 10 min from equation (10) considering the parameters given by the fitting curve.

Table 1 Weight-average molecular weight and zero-shear viscosity at various residence times

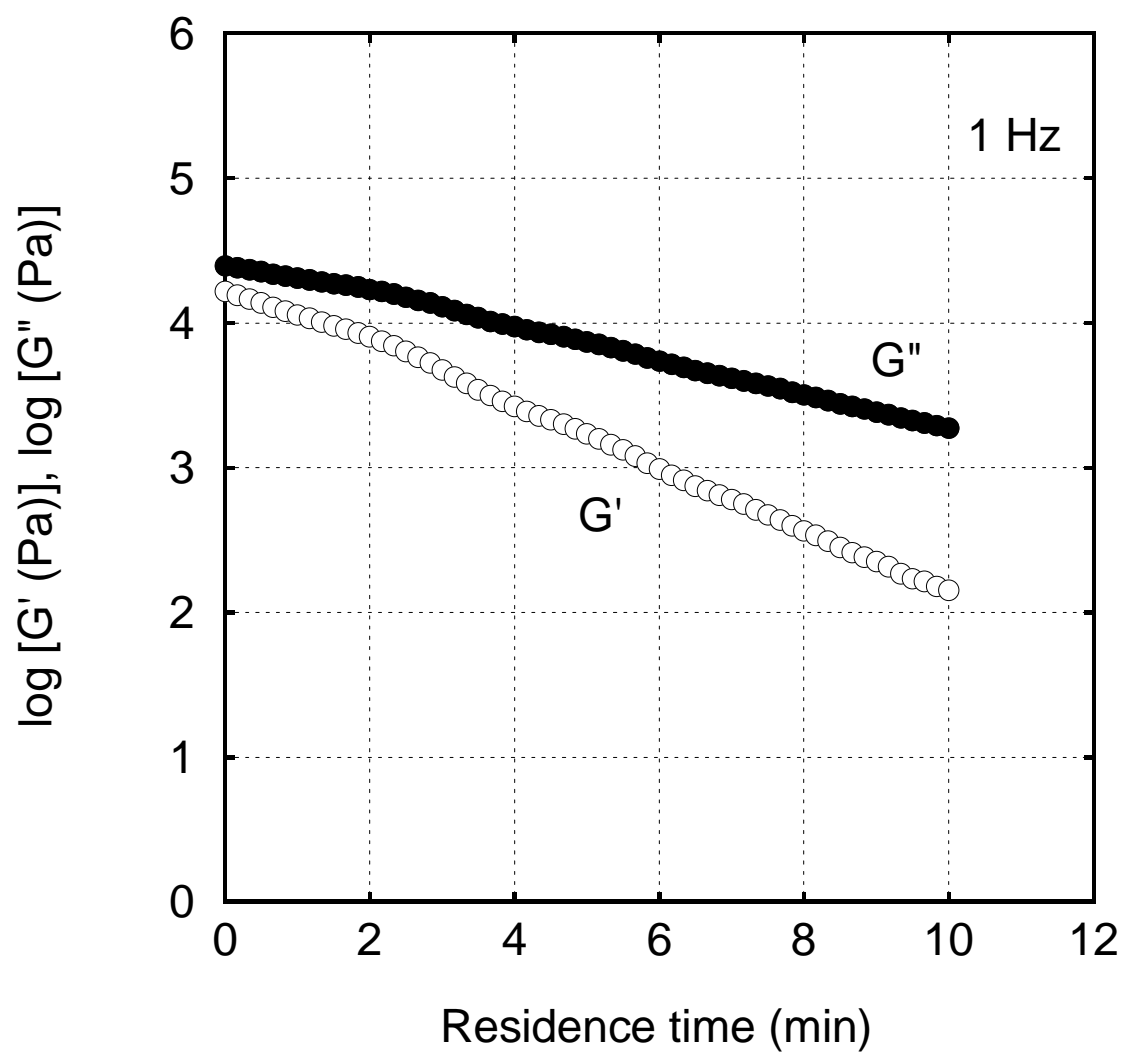
| Residence time in a rheometer (min) | Weight-average molecular weight, M_w | Zero-shear viscosity, η_0 (Pa s) |
|--|---|--|
| 0 | 434,000 | - |
| 5 | 302,000 | 1140 |
| 10 | 228,000 | 313 |

Figure 1(a)



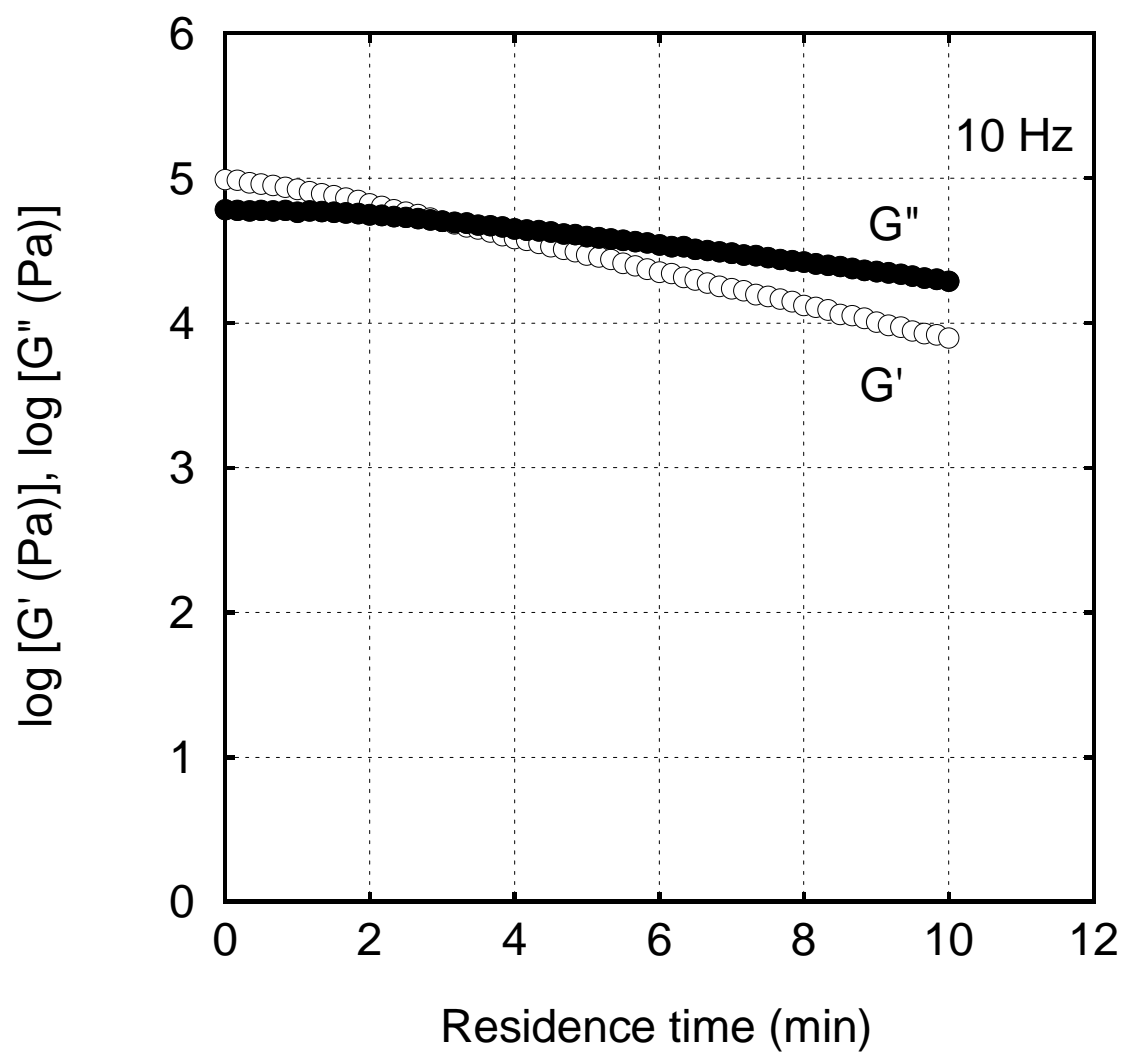
Residence time dependence of shear storage modulus G' (○) and loss modulus G'' (●) at 180 °C at 0.1 Hz for PHB.

Figure 1(b)



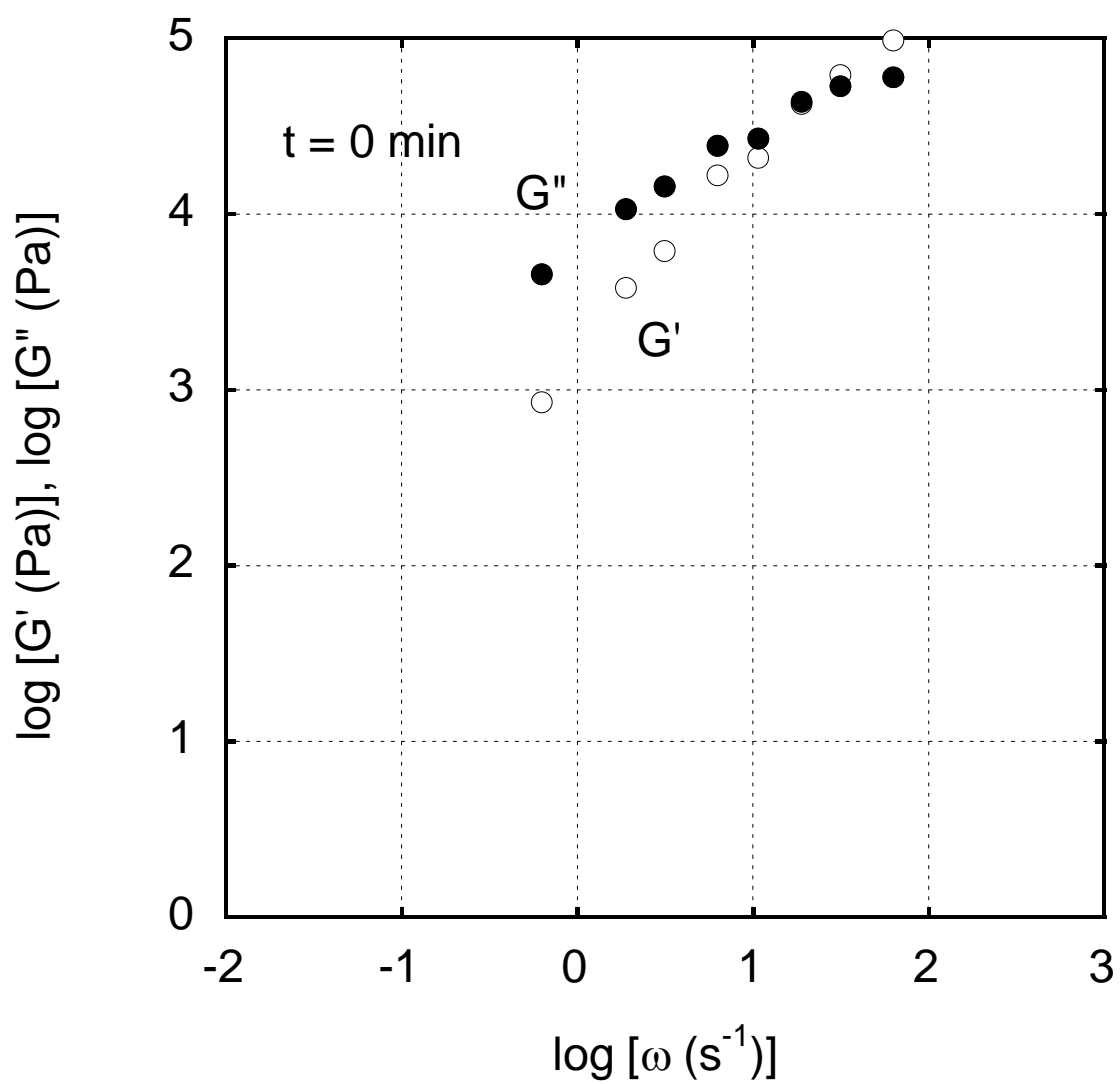
Residence time dependence of shear storage modulus G' (\circ) and loss modulus G'' (\bullet) at 180 °C at 1 Hz for PHB.

Figure 1(c)



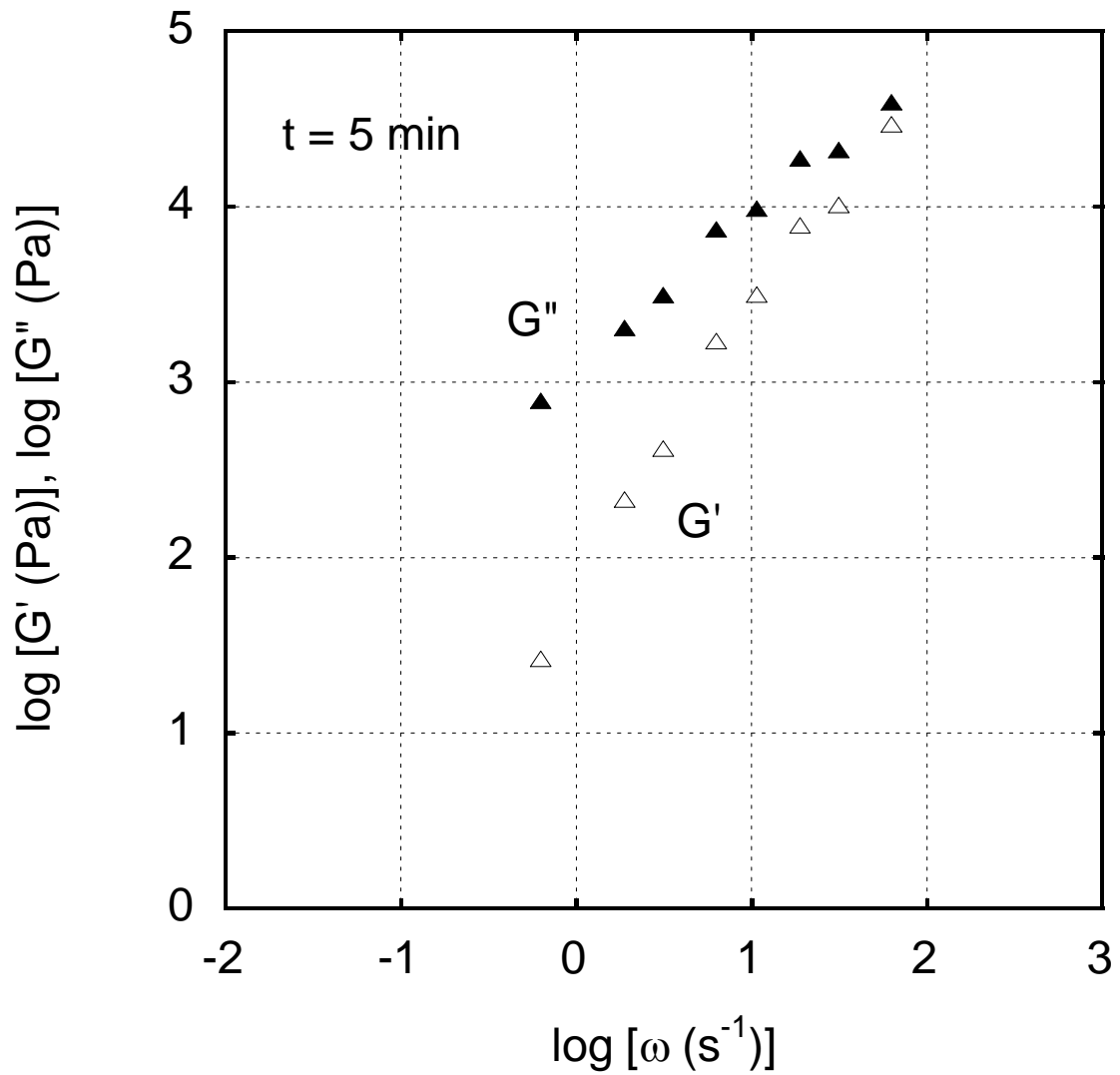
Residence time dependence of shear storage modulus G' (\circ) and loss modulus G'' (\bullet) at 180 °C at 10 Hz for PHB.

Figure 2(a)



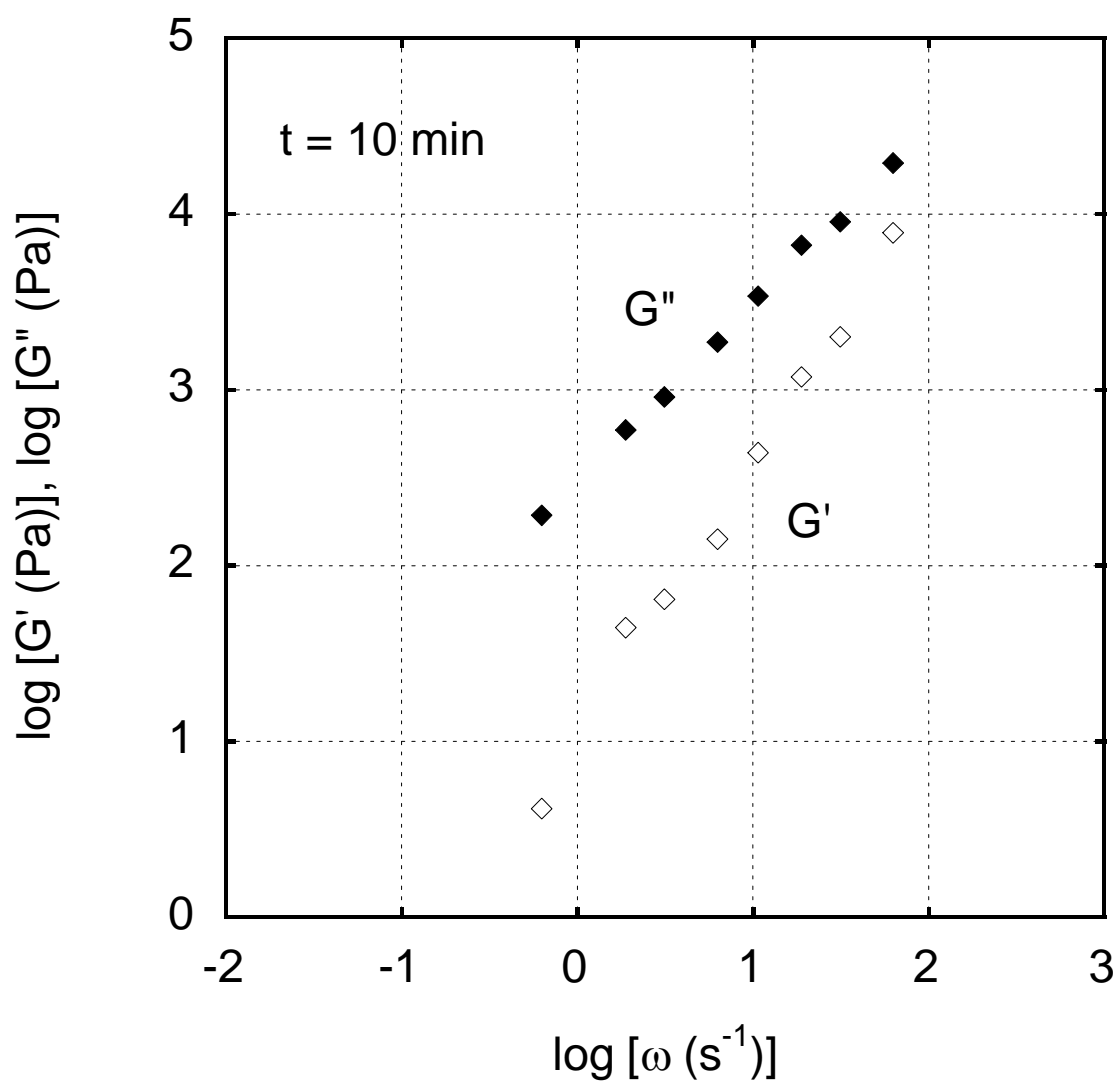
Shear storage modulus G' (\circ) and loss modulus G'' (\bullet) at 180 °C plotted against angular frequency ω for the samples with a residence time of 0 min in the rheometer.

Figure 2(b)



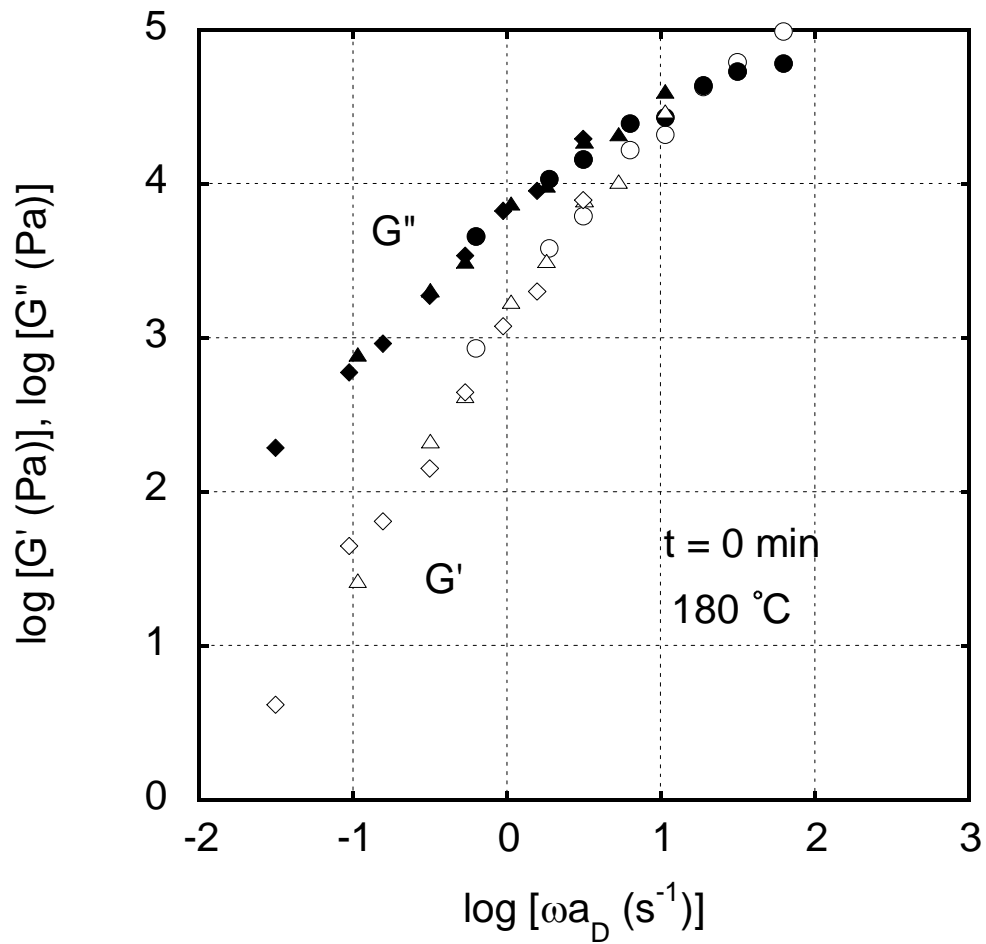
Shear storage modulus G' (Δ) and loss modulus G'' (\blacktriangle) at 180 °C plotted against angular frequency ω for the samples with a residence time of 5 min in the rheometer.

Figure 2(c)



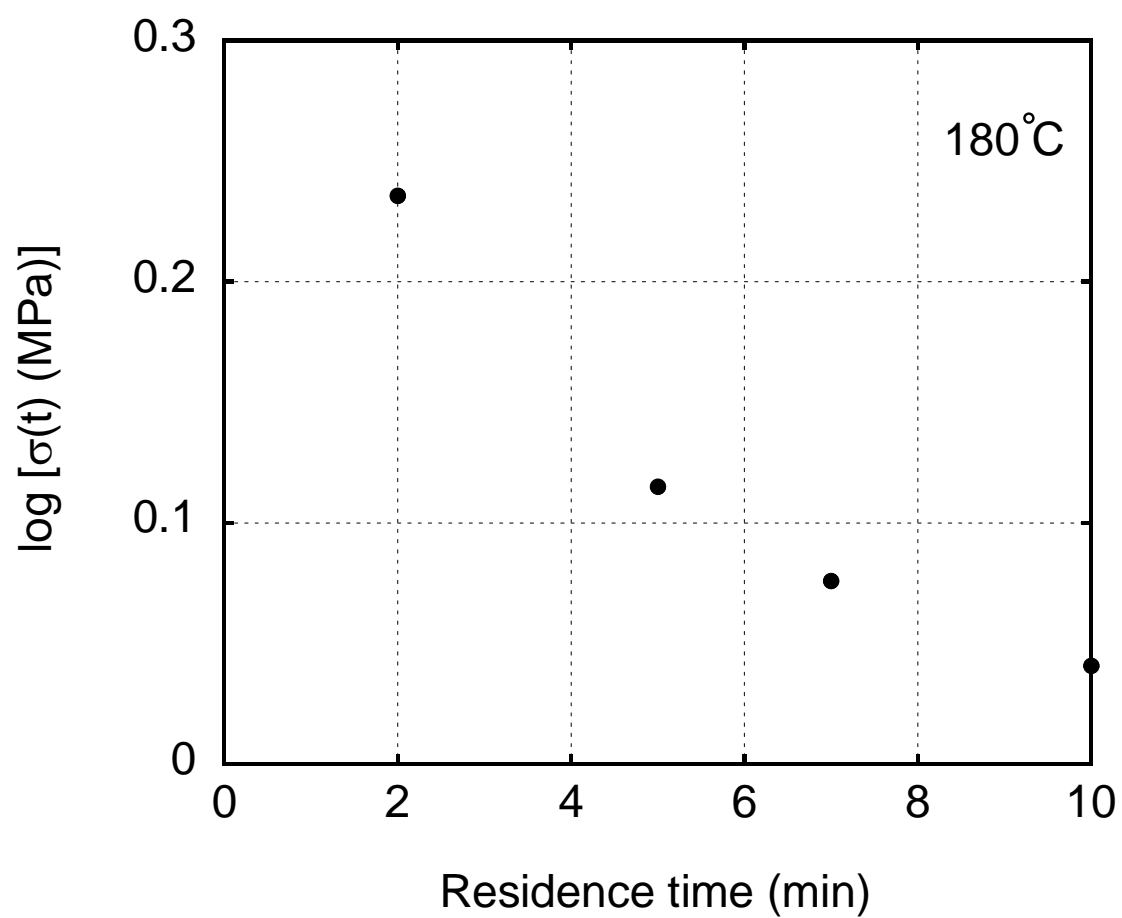
Shear storage modulus G' (\diamond) and loss modulus G'' (\blacklozenge) at 180 °C plotted against angular frequency ω for the samples with a residence time of 10 min in the rheometer.

Figure 3



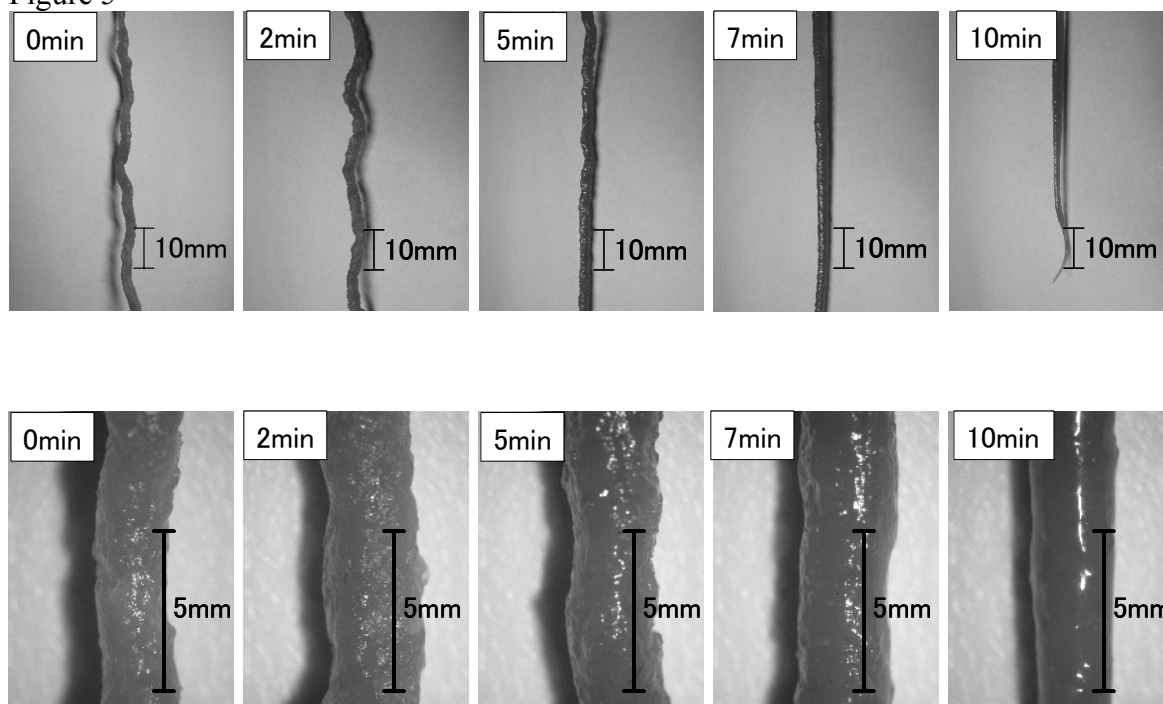
Master curves of shear storage modulus G' and loss modulus G'' at $180\text{ }^{\circ}\text{C}$ for the samples with various residence times, $t = 0, 5, 10$ min, in the rheometer; The symbols are the same as in Figure 2. a_D is the shift factor, and the residence time for the reference sample is 0 min, *i.e.*, $a_D = 1$.

Figure 4



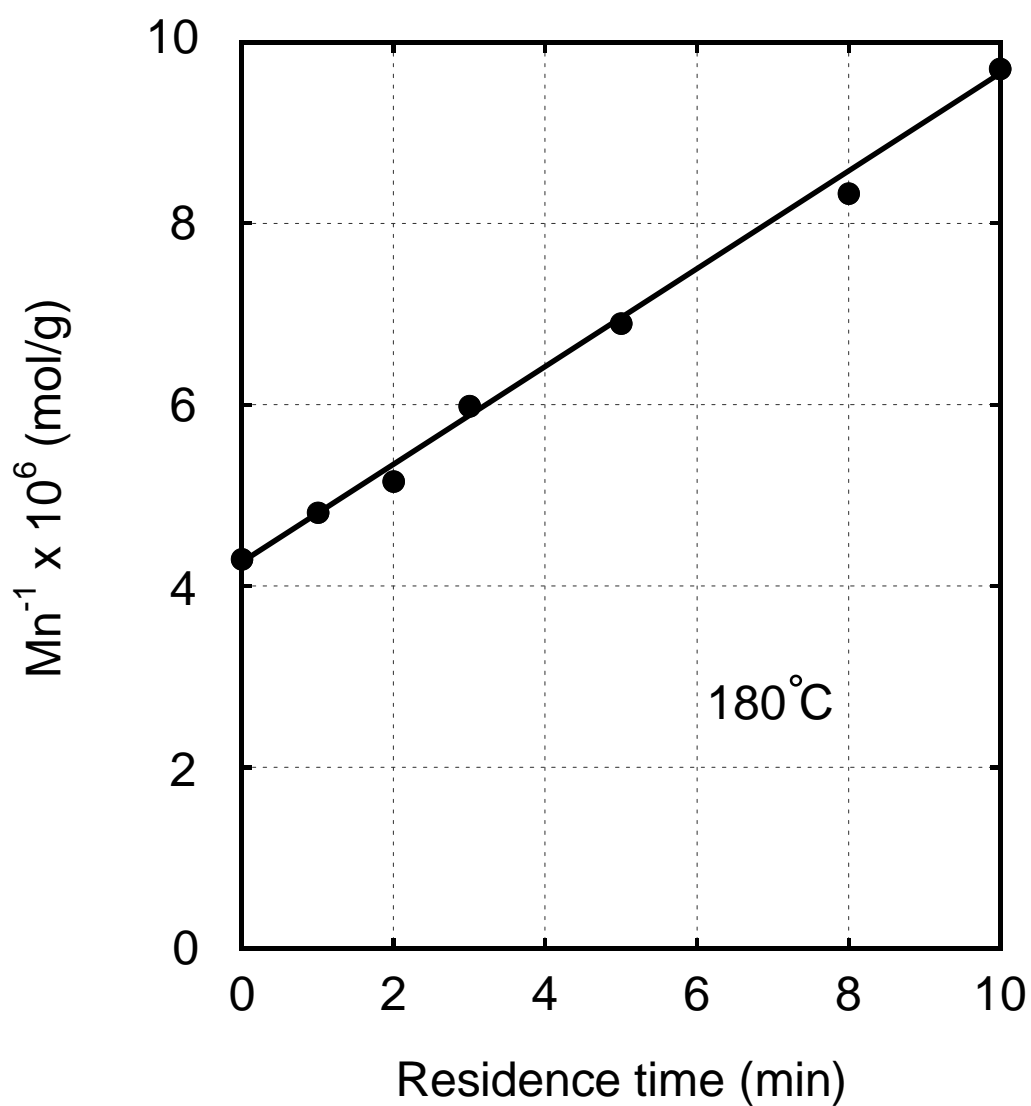
Apparent shear stress σ at a shear rate of 6.3 s^{-1} plotted against the residence time at $180 \text{ }^\circ\text{C}$.

Figure 5



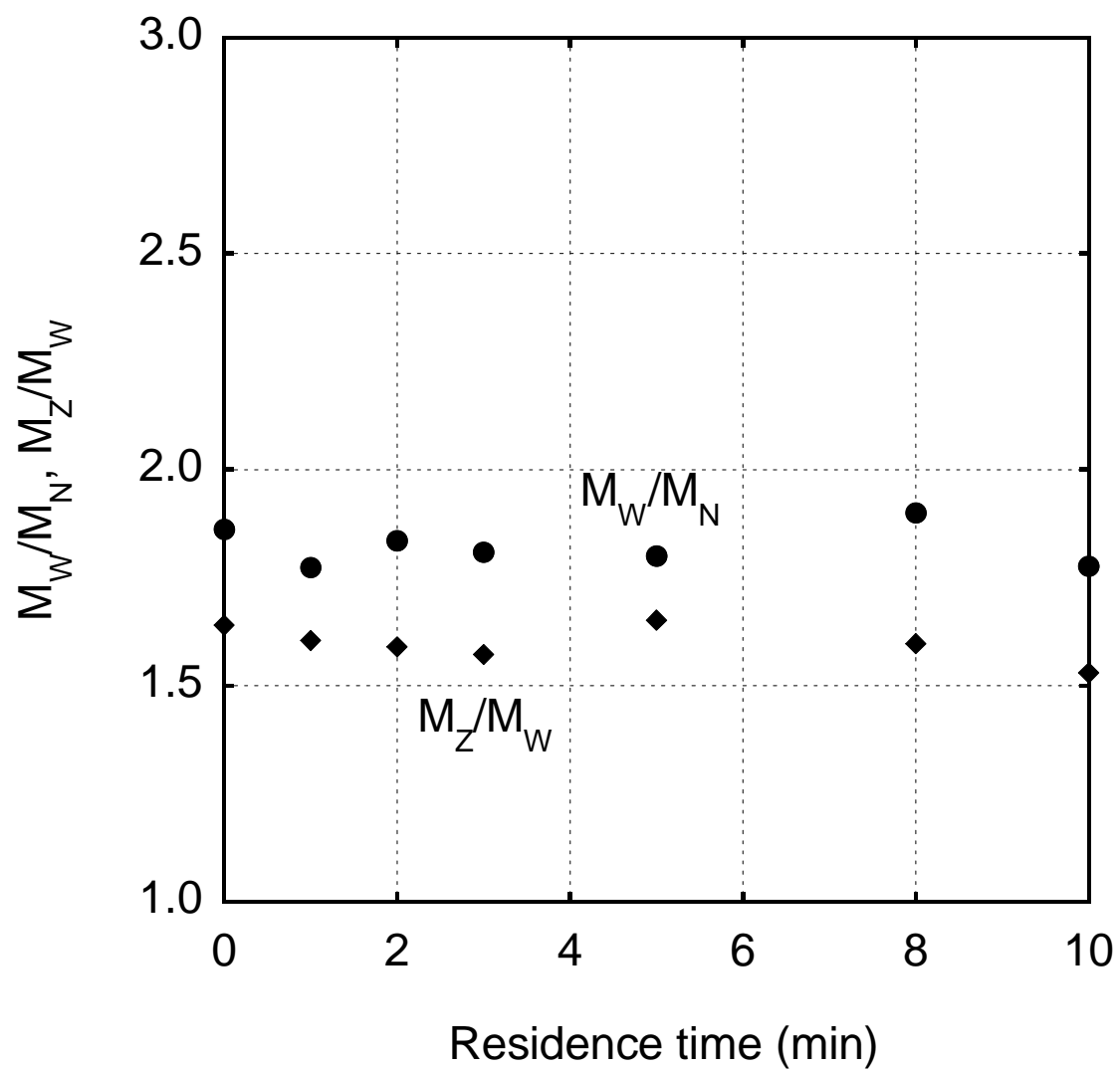
Optical photographs of strands extrudated from a capillary rheometer at a shear rate of 6.3 s^{-1} at $180 \text{ }^\circ\text{C}$ with various residence times.

Figure 6



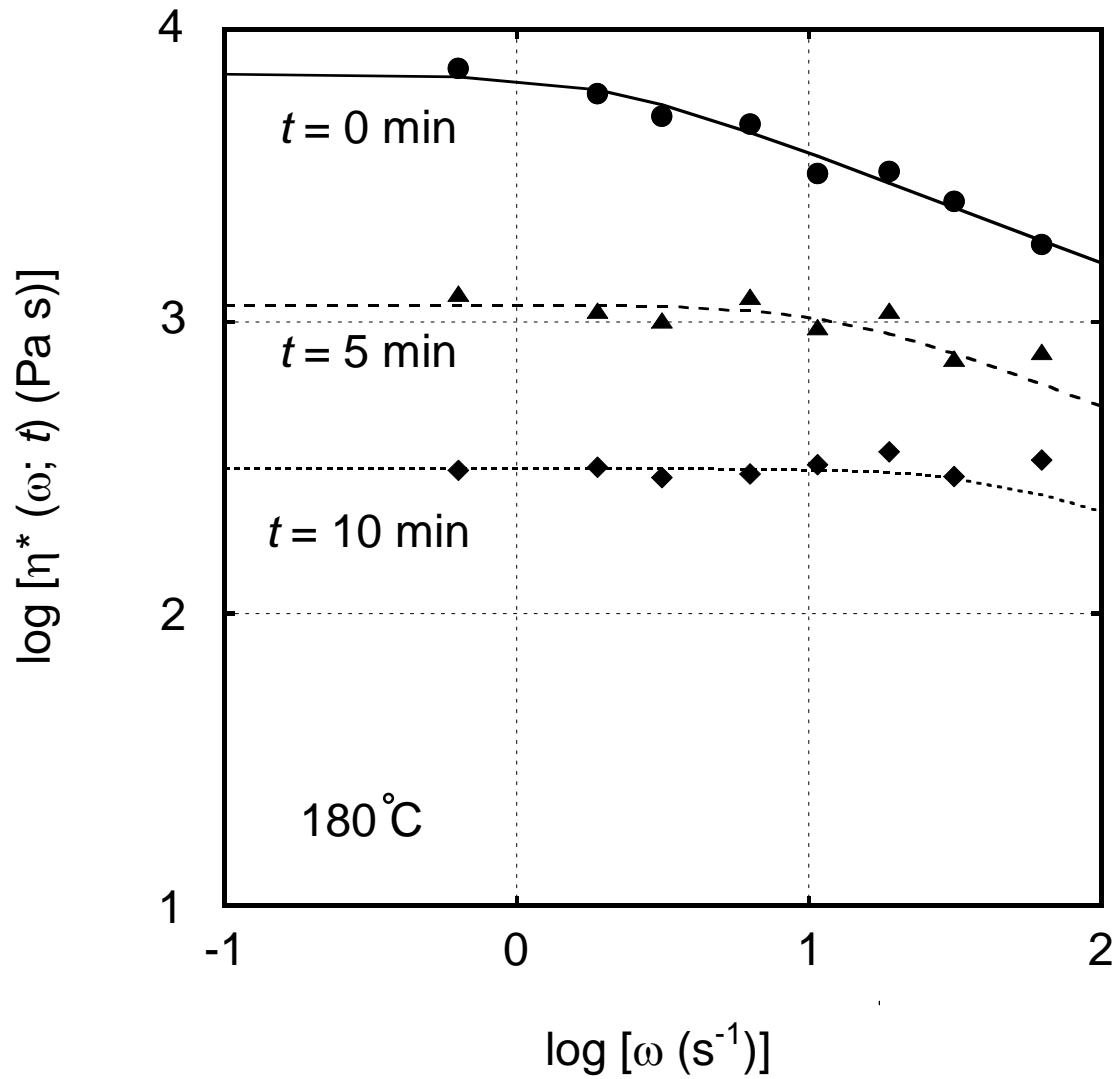
Inverse of number-average molecular weight, $1/M_N$, against the residence time in the rheometer at 180 °C.

Figure 7



Molecular weight distribution, such as (circles) M_w/M_N and (diamonds) M_z/M_w , as a function of the residence time.

Figure 8



Experimental data of absolute value of complex shear viscosity $\eta^*(\omega; t)$ for the sample with various residence times at 180 °C; circles $t = 0 \text{ min}$, triangles $t = 5 \text{ min}$, and diamonds $t = 10 \text{ min}$. In the figure, a fitting curve by equation (10) with $\eta_0(0) = 7000 \text{ [Pa s]}$ is represented by a solid line. The dotted lines are the predicted ones at $t = 5$ and 10 min from equation (10) considering the parameters given by the fitting curve.